C12-Helix Development in (αγ)n Sequences – Spectroscopic Characterization of Boc-[Aib-γ4(R)Val]-OMe Oligomers

Article *in* European Journal of Organic Chemistry · June 2013

DOI: 10.1002/ejoc.201300264

CITATIONS
9

READS
279

4 authors:

Dinesh Bhimareddy
French National Centre for Scientific Research
22 PUBLICATIONS **282** CITATIONS
SEE PROFILE

Vinaya Vishwanathan
Indian Institute of Science
2 PUBLICATIONS **16** CITATIONS
SEE PROFILE

S. Raghothama
Indian Institute of Science
122 PUBLICATIONS **3,001** CITATIONS
SEE PROFILE

Padmanabhan Balaram
Indian Institute of Science
595 PUBLICATIONS **19,813** CITATIONS
SEE PROFILE

DOI: 10.1002/ejoc.201300264

C_{12}-Helix Development in $(\alpha\gamma)_n$ Sequences – Spectroscopic Characterization of Boc–[Aib–γ^4(*R*)Val]–OMe Oligomers

Bhimareddy Dinesh,[a] Vishwanathan Vinaya,[b] Srinivasarao Raghothama,[b] and Padmanabhan Balaram*[a]

Keywords: Peptides / Amino acids / Helical structures / Conformation analysis

The solution conformations of the αγ-hybrid oligopeptides Boc–[Aib–γ^4(*R*)Val]$_n$–OMe (n = 1–8) in organic solvents have been probed by NMR, IR, and CD spectroscopic methods. In the solid state, this peptide series favors C_{12}-helical conformations, which are backbone-expanded analogues of 3_{10} helices in α-peptide sequences. NMR studies of the six- (n = 3) and 16-residue (n = 8) peptides reveal that only two NH protons attached the N-terminus residues Aib(1) and γ^4(*R*) Val(2) are solvent-exposed. Sequential N_iH–$N_{i+1}H$ NOEs characteristic of local helical conformations are also observed at the α residues. IR studies establish that chain extension leads to a large enhancement in the intensities of the hydrogen-bonded NH stretching bands (3343–3280 cm^{-1}), which suggest elongation of intramolecularly hydrogen-bonded structures. The development of C_{12}-helical structures upon lengthening of the αγ sequence is supported by the NMR and IR observations. The CD spectra of the $(\alpha\gamma)_n$ peptides reveal a negative maximum at ca. 206 nm and a positive maximum at ca. 192 nm, spectral feature that are distinct from those of 3_{10} helices in α-peptides.

Introduction

The area of foldamer research has exploded over the last few years, and many different approaches have been used to mimic structures of folded biological macromolecules by using non-native backbone structures.[1] The term "foldamer"[2] owes its origin to the finding that backbone-homologated amino acid residues, specifically β and γ, can be accommodated into folded polypeptide structures and indeed facilitate the generation of unprecedented hydrogen-bonded motifs in α-peptides.[3] A great deal of work on the design of folded peptides containing β and γ residues has focused on the use of conformationally constrained residues. Two distinct approaches have been employed to bias conformational choices ("pre-organization"). These are: (1) Cyclization to restrict one of the backbone C–C torsion angles close to the *gauche* conformation. (2) The introduction of geminal dialkyl substitution at one of the backbone carbon atoms, which limits the accessible range of flanking torsional angles.[4] Gellman has extensively demonstrated the utility of cyclic β-amino acids[5] and more recently γ residues[6] in the design of folded peptides with hybrid backbones. A recent report further illustrates the utility of cyclically constrained γ residues to generate peptide foldamers.[7] β-Amino acids bearing geminal dialkyl substituents and the achiral gabapentin (Gpn) residue, which is a β,β-disubstituted analog of γ-aminobutyric acid, have been extensively studied in our laboratory, and diverse hydrogen-bonded motifs have been structurally characterized.[8,3d] We wanted to check if conformational constraints are obligatory for the generation of stable foldamers of hybrid peptides with α, β, and γ residues. Stimulated by the early observations of Seebach[9] and Hanessian,[10] which suggested that short peptides containing γ residues, derived from genetically coded amino acids favor folded structures in solution, we began a systematic investigations of the conformational properties of unconstrained γ residues. New foldamer helical structures with mixed hydrogen-bonding directionality have been proposed for hybrid sequences containing a monosubstituted γ residue with a sugar-derived substituent at the γ position, on the basis of solution NMR.[11] These foldamer structures have also been supported by theoretical calculations.[12] In earlier reports, we have demonstrated the formation of stable folded helical structures in sequences of the type Boc–[Xxx–γ^4(*R*)Val]$_n$–OMe (Xxx = Aib or ^{L}Leu). C_{12}-helical structures in $(\alpha\gamma)_n$ sequences, which may be formally considered as backbone-expanded analogues of the classical 3_{10} helix of α-peptides, have been characterized in solids by X-ray diffraction for sequences up to 16 residues in length.[13] In this report, we describe the conformational properties of $(\alpha\gamma)_n$ foldamers in solution in the model sequences Boc–[Aib–γ^4(*R*)Val]$_n$–OMe (Figure 1). The γ^4(*R*)-Val residue is readily accommodated into folded helical peptide conformations in solution.

[a] Molecular Biophysics Unit, Indian Institute of Science, Bangalore 560012, India
Fax: +91-80-23600683
E-mail: pb@mbu.iisc.ernet.in
Homepage: http://mbu.iisc.ernet.in/~pbgrp/
[b] NMR Research Centre Indian Institute of Science, Bangalore 560012, India

Supporting information for this article is available on the WWW under http://dx.doi.org/10.1002/ejoc.201300264.

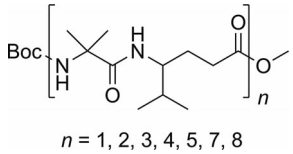

Figure 1. Boc–[Aib–γ^4(*R*)Val]$_n$–OMe.

Results and Discussion

Solution Conformations Probed by NMR Spectroscopy

NMR studies were performed at 500/700 MHz with $CDCl_3$ solutions. Intramolecular hydrogen bonding is promoted in organic solvents and allows estimation of the tendency of designed sequences to fold into well-ordered structures. Previous crystallographic studies have demonstrated the formation of $\alpha\gamma$ C_{12} helices for four- (n = 2), eight- (n = 4), 10- (n = 5), and 16-residue (n = 8) peptides.[13a] The NMR discussion below is restricted to the six-residue sequence (n = 3), for which a crystal structure is not available, and the 16-residue sequence (n = 8), which has been structurally characterized by X-ray crystallography. Figure 2 shows the ^{1}H NMR spectra of the six- and 16-residue peptides Boc–[Aib–γ^4(*R*)Val]$_n$–OMe (n = 3 and 8) in $CDCl_3$. In both peptides, extremely well dispersed resonances were observed for the backbone NH protons.

Sequence-specific assignments were performed by using a combination of TOCSY and ROESY experiments and were facilitated by the unambiguous assignments of the upfield shifted urethane NH proton of Aib(1). TOCSY connectivities across the γ residues are critical, as the N_iH–$N_{i+1}H$ distance of γ residues can be greater than 3.5 Å, which results in weak or unobserved d_{NN} NOEs. The chemical-shift dispersion for the 16-residue peptide facilitated experiments to delineate intramolecularly hydrogen-bonded NH groups. Figure 3 summarizes the variation of NH proton chemical shifts upon addition of the hydrogen-bonding solvent [D_6]DMSO to solutions of peptides in $CDCl_3$. This solvent titration experiment permits a facile distinction between solvent-exposed (free) and solvent-shielded (hydrogen-bonded) NH groups. Accessible NH groups readily interact with [D_6]DMSO, which results in pronounced downfield shifts of their resonances as the concentration of the cosolvent increases, whereas buried NH groups show a little or no dependence of NH chemical shifts on cosolvent concentration. Inspection of Figure 3 reveals that in both peptides only the two N-terminal NH groups Aib(1) and γ(*R*)Val(2) are solvent-exposed. This observation strongly suggests that all the remaining NH groups are involved in intramolecular hydrogen bonding, a feature that is consistent with the formation of a continuous C_{12} helix. Figure 4 shows the partial ROESY spectra corresponding to d_{NN} NOEs in the six- and 16-residue peptides. It is evident that $d_{N_iN_{i+1}}$ NOEs are strong and readily observed for the Aib residues, whereas the corresponding NOEs are significantly weak or unobserved for the γ residues. Interestingly, the $d_{N_iN_{i+1}}$ NOE is observed for the γ(*R*)Val(2) residue in both peptides. The determination of the sequential interproton distances in the crystal structure of the 16-residue peptide

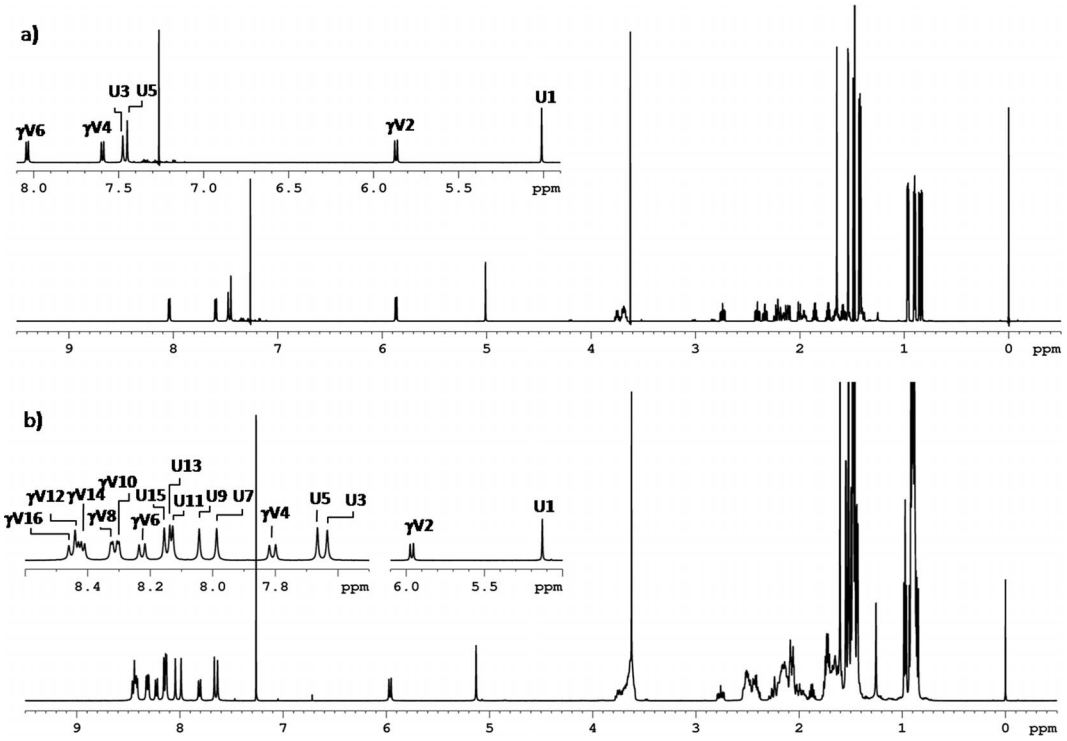

Figure 2. ^{1}H NMR spectra of peptides in $CDCl_3$ at 305 K: (a) Boc–[Aib–γ^4(*R*)Val]$_3$–OMe (700 MHz) and (b) Boc–[Aib–γ^4(*R*)Val]$_8$–OMe (500 MHz). The inset shows an expansion of the amide NH resonances. U = Aib, γV = γ^4(*R*)Val.

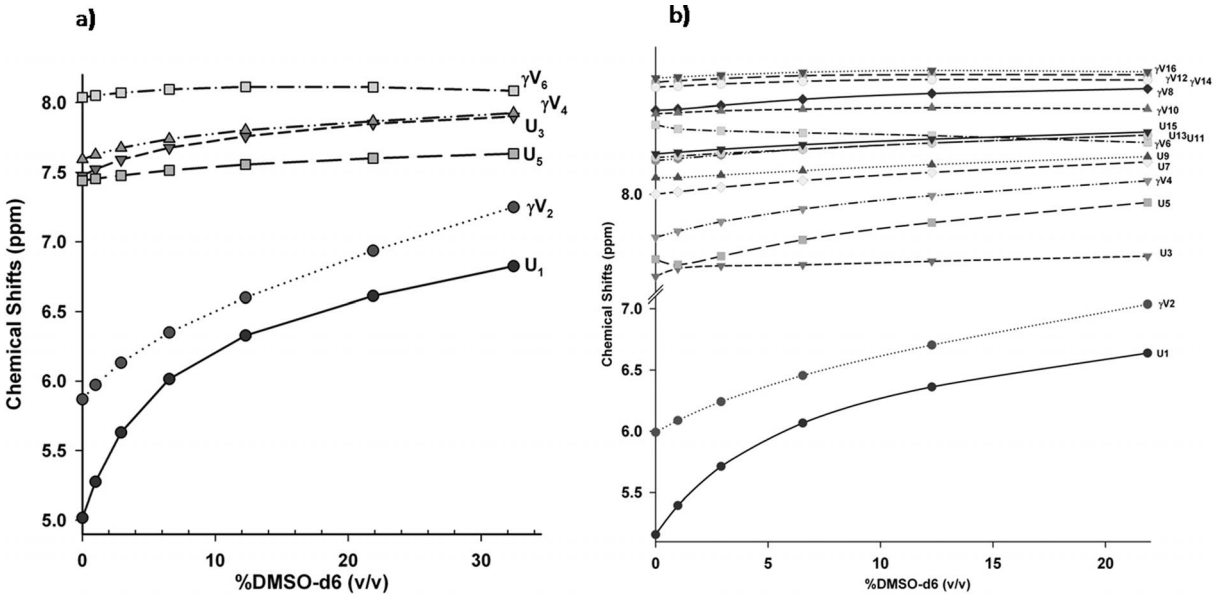

Figure 3. Dependence of NH chemical shifts as a function of [D_6]DMSO concentration in $CDCl_3$/[D_6]DMSO mixtures for the peptides (a) Boc–[Aib–γ^4(*R*)Val]$_3$–OMe and (b) Boc–[Aib–γ^4(*R*)Val]$_8$–OMe. U = Aib, γV = γ^4(*R*)Val.

yielded average values of ca. 2.85 Å for Aib and ca. 3.75 Å for γ(*R*)Val. Interestingly, one of the shortest distances (3.61 Å) is for the γ(*R*)Val(2) residue. A notable feature of the spectra in Figure 4 is the $d_{N_i-N_{i+2}}$ NOE at the N-terminus of the 16-residue peptide. Two distinct $N_iH–N_{i+2}H$ correlations corresponding to Aib(1)↔Aib(3) and γVal(2)↔γVal(4) are observed, although their intensities are significantly less intense than those of the sequential NOEs. In the C_{12} helix crystallographically characterized for this peptides, the corresponding interproton distances are 4.47 and 4.53 Å, which should normally preclude observation of NOEs. It is likely that these NOEs are from a population of structures involving the three residue, αγα or γαγ, which are α-turn homologues.[3d,14] The solvent titration experiments, together with the observation of $d_{N_i-N_{i+1}}$ NOEs, supports the formation of a C_{12}-helical structure in solution in both peptides. In the C_{12}-helical structure formed by the sequence Boc–[Aib–γ^4(*R*)Val]$_n$–OMe, NOEs of the type $C^\gamma H_i \leftrightarrow NH_{i+2}$ may be anticipated.[6a] Unfortunately, in this series the γ^4(*R*)Val $C^\gamma H$ protons overlap, which precludes the observation of their NOEs.

IR Spectroscopy

IR studies were performed with $CHCl_3$ solutions at peptide concentrations of 2 mM. Preliminary experiments with the eight-residue (n = 4) peptide indicated an absence of concentration dependence even up to 8 mM. Table 1 summarizes the observed frequencies for the amide-group vibrations. Figure 5 (a) shows the N–H stretching bands (3500–3200 cm^{-1}) for the peptides Boc–[Aib–γ^4(*R*)Val]$_n$–OMe (n = 1–8). In the dipeptide ester, Boc–Aib–γ^4(*R*)Val–OMe, only one N–H stretching band is observed at 3434 cm^{-1}, which corresponds to a non-hydrogen-bonded NH group (ν^f_{NH}). As the chain length increases, the appearance of a second N–H stretching band at 3343 cm^{-1} is observed for the tetrapeptide ester Boc–[Aib–γ^4(*R*)Val]$_2$–OMe.

Table 1. IR stretching frequencies for peptides Boc–[Aib–γ^4(*R*)-Val]$_n$–OMe (n = 1–8) in chloroform.

Peptide (n)	ν_{NH} [cm^{-1}] Free	H-bonded	Amide I [cm^{-1}]	Amide II [cm^{-1}]	(ν_{CO}) Urethane [cm^{-1}]
1	3434	–	1728	1494	–
2	3426	3343	1673	1530	1712
3	3424	3319	1661	1541	1709
4	3423	3308	1655	1543	1708
5	3422	3296	1651	1545	1708
7	3422	3285	1649	1548	1707
8	3424	3280	1648	1549	1708

The appearance of the new band at low frequency is attributed to hydrogen-bonded NH groups (ν^{hb}_{N-H}). The data in Figure 5 (a) clearly reveals that as the chain length increases, the intensity of the hydrogen-bonded N–H band increases dramatically; this suggests that the increase in peptide chain length is accompanied by an increase in the number of hydrogen-bonded NH groups. Taken together with X-ray and NMR analysis of the peptides in this series, the IR data strongly supports the formation of C_{12}-helical structures even in the shorter sequences, beginning at the level of the tetrapeptide. The amide I (C=O stretch) band shifts to lower frequencies from the four-residue peptide (1673 cm^{-1}) to the 16-residue peptide (1648 cm^{-1}). The low-frequency shift appears to level off after a length of 10 residues is reached. Similar studies were reported over three decades ago, and the development of 3_{10}-helical structures was examined in peptide sequences derived from a membrane-active peptide alamethicin, which were rich in Aib residues.[15]

Lengthening of the C_{12} helical structure in these sequences should in principle lead to a regular variation of

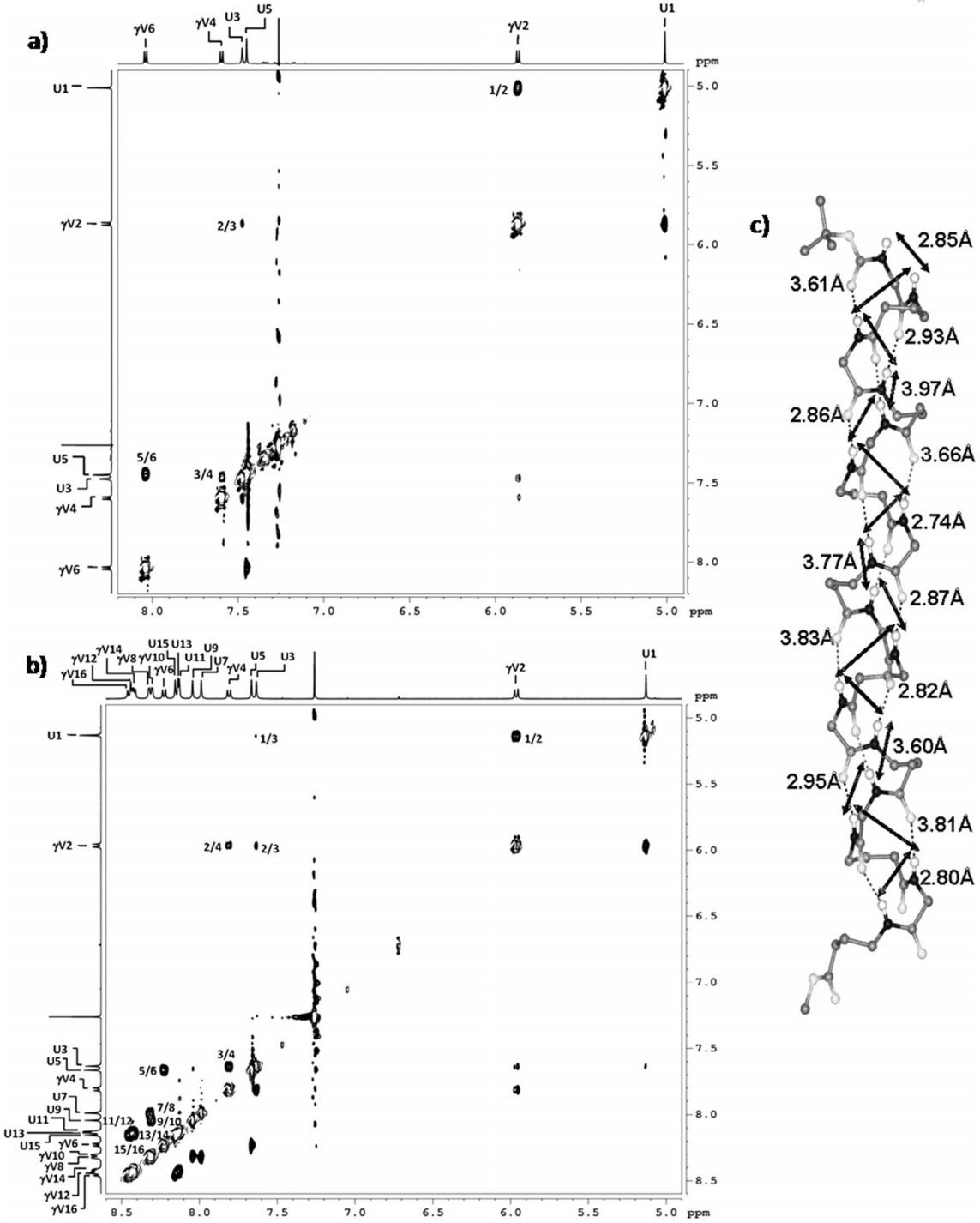

Figure 4. Partial ROESY spectra of the peptides (a) Boc–[Aib–γ^4(*R*)Val]$_3$–OMe and (b) Boc–[Aib–γ^4(*R*)Val]$_8$–OMe at 305 K, observed d_{NN} NOEs are marked. (c) Sequential ($d_{N_i-N_{i+1}}$) distances in the crystal structure of the peptide Boc–[Aib–γ^4(*R*)Val]$_8$–OMe are indicated. The average values observed are $d_{N_i-N_{i+1}}$ (α) = 2.85 Å and $d_{N_i-N_{i+1}}$ (γ) = 3.6 Å. U = Aib, γV = γ^4(*R*)Val.

properties that depend on peptide shape and accessible surface area. Figure 5 (b) shows a plot of the retention factor of the Boc–[Aib–γ^4(*R*)Val]$_n$–OMe peptides on a reversed-phase C_{12} HPLC column. A satisfactory linear correlation with chain length is observed, which suggests that chain extension leads to a largely uniform development of a C_{12}-helical structure along the length of the molecule.

Circular Dichroism

Although a large body of literature exists on the characterization of helical peptide structures in α-peptide sequences by CD spectroscopy,[16] there are relatively few reports on CD spectra of well-defined hybrid oligopeptide sequences.[17] The availability of peptides in the Boc–[Aib–

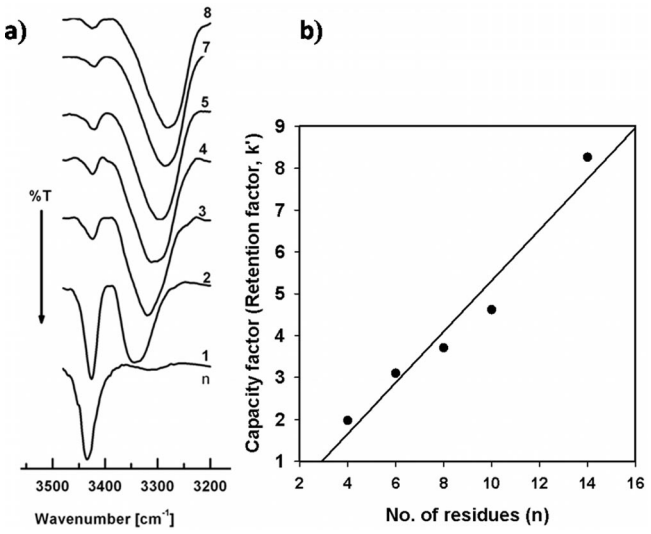

Figure 5. (a) IR spectra in the region 3500–3200 cm^{-1} for the peptides Boc–[Aib–γ^4(*R*)Val]$_n$–OMe (n = 1–8) in $CHCl_3$ at 2 mM concentration. (b) Variation of HPLC retention factor on a reversed-phase Jupiter Proteo C_{12} column (10–250 mm, 4 m particle size) for the peptides Boc–[Aib–γ^4(*R*)Val]$_n$–OMe (n = 2, 3, 4, 5, 7) with methanol/water gradients of 85–99% (methanol) at a flow rate of 2.5 mL/min and a 45 min run.

γ^4(*R*)Val]$_n$–OMe series presents an opportunity to examine the effect of increasing chain length in structurally well-characterized $(\alpha\gamma)_n$ sequences. Figure 6 shows an overlay of the electronic CD spectra (CD spectra for individual peptides are provided in the Supporting Information) of the peptides with chain lengths of 4–16 residues. The positions of the CD bands and their intensities are summarized in Table 2. Lengthening the peptide chain leads to the anticipated increase in molar ellipticity. Two distinct CD bands are observed in the longer sequences (10–16 residues). There is a negative maximum at 206 nm and a positive maximum at 191–192 nm. There is a small redshift of both bands in the shorter peptides. These spectral features may be contrasted with those observed for model 3_{10}-helical peptides in all α sequences, for which a distinct band is observed at ca. 220–222 nm, which intensifies in α-helical sequences.[16]

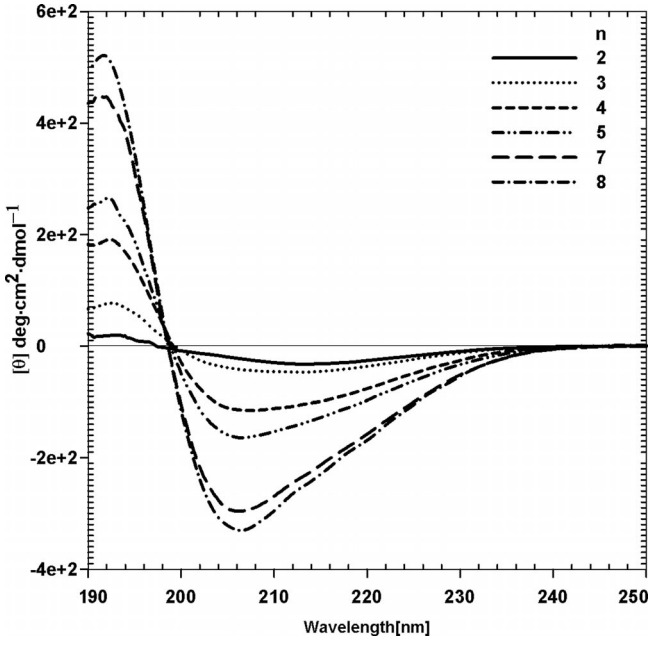

Figure 6. Overlay of the electronic CD (ECD) spectra of the peptides Boc–[Aib–γ^4(*R*)Val]$_n$–OMe (n = 2–8). Solvent: trifluoroethanol (TFE), $T \approx 298$ K.

Table 2. CD Parameters for peptides Boc–[Aib–γ^4(*R*)Val]$_n$–OMe (n = 2–8) in trifluoroethanol (TFE).

Peptide (n)	Conc. [mM]	θ_{-max} [deg cm^2 dmol^{-1}]	λ [nm]	θ_{+max} [deg cm^2 dmol^{-1}]	λ [nm]
2	0.8	–32500	213	20000	193
3	0.65	–47108	213	77143	193
4	0.45	–114800	207	191714	192
5	0.3	–166429	206	265714	192
7	0.25	–298571	206	455429	191
8	0.15	–334286	206	524000	192

Indeed, the 222 nm band has been ascribed to the n–π* electronic transition, and the two shorter wavelength bands with opposite signs have been assigned to the exciton split components of the π–π* transition. The interaction between amide chromophores in C_{12}-helical structures is undoubtedly different from that in the analogous C_{10} (3_{10}) helical structures. Future theoretical and experimental investigations are required to clarify the spectral signatures of hybrid helices.

Conclusions

A great deal of recent literature in the area of peptide foldamers with hybrid backbones has centered on the use of conformationally constrained β and γ residues.[5,6,8] Indeed, much of our work in this area focused on the β,β-disubstituted γ-amino acid residue gabapentin,[8] based on the knowledge that *gem*-dialkyl substitution would restrict the flanking torsion angles C^γ–C^β (θ_1) and C^β–C^α (θ_2) to *gauche* (g^+/g^-, $\theta \approx \pm 60°$) conformations, which are required for local folding of the peptide backbone. Ironically, more recent work with unconstrained γ-amino acid residues derived by homologation of the genetically coded α-amino acid residues suggests that unconstrained γ residues bearing a single substituent at the γ position (C_4) have an intrinsic tendency to form folded structures.[13,18] The question arises as to the extent to which the conformationally constrained α-amino acid Aib contributes to the observed C_{12}-helical folding patterns in the αγ-hybrid sequences. We have previously reported that replacement of Aib by Leu in short hybrid sequences of the type αγα and $(\alpha\gamma\alpha)_2$ does not affect folded C_{12} hydrogen-bonded structures in the solid state. Indeed the formation of crystals yielding well-defined incipient C_{12}-helical structures in short $(\alpha\gamma)_n$ sequences was surprising in view of the difficulties in characterizing short helical segments in α-peptides in the absence of stereochemically constrained residues.[13b] The ability to use chiral, uncon-

strained γ residues offers the possibility to expand the scope of hybrid foldamer design to address the specific problems of spectroscopic characterization of new helical structures in solution.

We have presented NMR, IR, and CD spectroscopic data for a series of $(\alpha\gamma)_n$ peptides, for which C_{12}-helical conformations have been demonstrated in the crystalline state. The NMR results clearly establish that longer chains result in an extension of the C_{12}-helical fold, and successive C terminal NH groups are involved in intramolecular hydrogen bonding. This progressive increase in the number of intramolecular hydrogen-bonded NH groups with chain length is also confirmed by the IR data, in which the N–H stretching bands are used as a probe. The results strongly suggests that in the Boc–[Aib–γ^4(*R*)Val]$_n$–OMe series the crystallographically observed C_{12} helices are also predominant in solution. The C_{12} helix may be derived from the classical 3_{10} helix by inserting a CH_2–CH_2 moiety into the backbone of alternate residues along the sequence. The type III β-turn, which is a two-residue (αα, C_{10}) conformational feature in peptides is then expanded to a C_{12}-helical turn. The preliminary CD data presented in this report suggest that the characteristic spectral features of the C_{12} helix differ significantly from those of the 3_{10} (C_{10}) helix, presumably as a result of variation in interchromophore distances. The ability to insert additional methylene groups in a controllable manner into well-defined secondary structures should prove valuable in peptide foldamer design.

Experimental Section

General: Boc–γ^4(*R*)Val–OH was synthesized by previously described procedures. All peptides were prepared by solution-phase synthesis by using the Boc group for N-terminal protection. The C terminus was protected as a methyl ester. Deprotections were performed by using 98% formic acid to remove the Boc group, whereas the methyl ester was removed by alkaline hydrolysis. Couplings were mediated by isobutylchloroformate (IBCF) for dipeptides and with *O*-(7-azabenzotriazol-1-yl)-*N*,*N*,*N*′,*N*′-tetramethyluronium hexafluorophosphate (HATU) and 1-hydroxy-1*H*-benzotriazole (HOBt) for longer sequences. All intermediates were characterized by ESI-MS and TLC on silica gel [$CHCl_3$/MeOH, 9:1 v/v)] and were used without further purification. The final peptides were obtained as pure products after they had been washed with hexane/diethyl ether mixtures. The purity of the final peptides was assessed by using reversed-phase HPLC with a Jupiter Proteo C_{12} column (10–250 mm, 4 m particle size) and methanol/water systems, monitored at 226 nm. Melting points were determined with a Stuart melting point apparatus SMP10. CD spectra were recorded with a JASCO J-715 spectropolarimeter with samples in trifluoroethanol (TFE), a path length of 1 mm, and a scanning speed of 20 nm/min. Peptide concentrations were in the range 0.8–0.15 mM. ESI-MS was performed with a Bruker Daltonics Esquire-3000 instrument, and ^{1}H NMR spectra were recorded with Bruker 500 MHz or 700 MHz spectrometers. IR spectra were recorded with a Perkin–Elmer 781 spectrometer with NaCl cells of path length 0.1 mm and 2 mM $CHCl_3$ solutions.

Boc–Aib–γ^4(*R*)Val–OMe (*n* = 1): Boc–Aib–OH (2.5 g, 12.3 mmol) was dissolved in dichloromethane (DCM, 40 mL), and the solution was cooled in an ice/salt bath. *N*-Methylmorpholine (NMM, 1.42 mL, 12.9 mmol) and IBCF (1.75 mL, 13.5 mmol) were added as the reaction mixture was stirred. After 10 min, a precooled solution of HCl·H–Val–OMe (2.4 g, 12.3 mmol) and NMM (1.35 mL, 12.3 mmol) was added. The pH of the solution was adjusted to ca. 8 by adding NMM, and the reaction mixture was stirred overnight at room temperature. DCM (100 mL) was added to the reaction mixture, which was washed successively with brine (3× 50 mL), 10% $KHSO_4$ (3× 50 mL), 50% $NaHCO_3$ (3× 40 mL), and water. The combined organic layer was dried with anhydrous sodium sulfate, and the solvents were evaporated. The yellow oil was triturated with hexane (2× 10 mL) to yield Boc–Aib–γ^4(*R*)-Val–OMe (3.6 g, 85%) as a white solid, m.p. 136–137 °C. MS (ESI): 345.3 $[M + H]^+$, 367.3 $[M + Na]^+$, 383.1 $[M + K]^+$.

Boc–[Aib–γ^4(*R*)Val]$_2$–OMe (*n* = 2): Boc–Aib–γ^4(*R*)Val–OMe (1 g, 2.91 mmol) in tetrahydrofuran (THF) /water (7/8 mL) was cooled in and ice bath, and a NaOH solution (0.15 g, 3.75 mmol in 1 mL of water) was added dropwise. The ice bath was removed, and the reaction mixture was stirred until TLC indicated complete consumption of the starting material (30 min). Acidification to pH ≈ 2 with $KHSO_4$ was followed by extraction with DCM (50 mL). The aqueous layer was further extracted with DCM (3× 20 mL), and the combined organic fractions were dried with Na_2SO_4 and concentrated under vacuum to yield Boc–Aib–γ^4(*R*)Val–OH (0.94 g, 98%) as a white solid, which was used for further reactions without purification. Boc–Aib–γ^4(*R*)Val–OMe (1 g, 2.91 mmol) was deprotected with 98% formic acid (5 mL), and the reaction was monitored by TLC. After 4 h, the formic acid was evaporated, and the residue was dissolved in water (10 mL). The pH of the aqueous layer was adjusted to ca. 8 by the addition of sodium carbonate, and the mixture was extracted with DCM (3× 30 mL). The combined organic layer was washed with brine (30 mL) and concentrated under vacuum to a volume of ca. 2 mL. The dipeptide free base was added to a precooled solution of Boc–Aib–γ^4(*R*)Val–OH (0.94 g, 2.85 mmol) in DCM (10 mL) and *N*,*N*-dimethylformamide (DMF, 2 mL), and HATU (1.1 g, 2.85 mmol) and HOBt (0.436 g, 2.85 mmol) were added. The reaction mixture was allowed to attain room temperature and was stirred for 6 h. The reaction was worked up as detailed for Boc–Aib–γ^4(*R*)Val–OMe. Boc–[Aib–γ^4(*R*)Val]$_2$–OMe (1.4 g, 88%) was obtained as a white solid, m.p. 162–164 °C. MS (ESI): 557.2 $[M + H]^+$, 579.2 $[M + Na]^+$, 595.1 $[M + K]^+$.

Boc–[Aib–γ^4(*R*)Val]$_3$–OMe (*n* = 3): Boc–[Aib–γ^4(*R*)Val]$_2$–OMe (0.5 g, 0.9 mmol) was deprotected with 98% formic acid (3 mL) and was worked up as described for Boc–[Aib–γ^4(*R*)Val]$_2$–OMe. The free base was added to a precooled solution of Boc–Aib–γ^4(*R*)-Val–OH (0.296 g, 0.9 mmol), obtained as described for Boc–[Aib–γ^4(*R*)Val]$_2$–OMe, in DCM (15 mL) and DMF (4 mL), and HATU (0.34 g, 0.9 mmol) and HOBt (0.137 g, 0.9 mmol) were added. The reaction mixture was allowed to attain room temperature and was stirred for 6–7 h. The reaction was worked up as described for Boc–Aib–γ^4(*R*)Val–OMe. Boc–[Aib–γ^4(*R*)Val]$_3$–OMe was obtained as a white solid (0.6 g, 87%), m.p. 225–227 °C. MS (ESI): 769.1 $[M + H]^+$, 791.1 $[M + Na]^+$, 807.1 $[M + K]^+$.

Boc-[Aib-γ^4(*R*)Val]$_4$-OMe (*n* = 4): Boc–[Aib–γ^4(*R*)Val]$_2$–OMe (0.35 g, 0.63 mmol) was deprotected with 98% formic acid (3 mL) and was worked up as described for Boc–[Aib–γ^4(*R*)Val]$_2$–OMe. The free base was added to a precooled solution of Boc–[Aib–γ^4-(*R*)Val]$_2$–OH, obtained as described for Boc–[Aib–γ^4(*R*)Val]$_2$–OMe, in DCM (15 mL) and DMF (5 mL), and HATU (0.24 g, 0.629 mmol) and HOBt (0.96 g, 0.629 mmol) were added. The reaction mixture was allowed to attain room temperature and was stirred for 6–7 h. The reaction was worked up as described for Boc–Aib–γ^4(*R*)Val–OMe. Boc–[Aib–γ^4(*R*)Val]$_4$–OMe was obtained as a

white solid (0.55 g, 89%), m.p. 232–234 °C. MS (ESI): 981.1 $[M + H]^+$, 1003.1 $[M + Na]^+$, 1019.0 $[M + K]^+$.

Boc–[Aib–γ^4(*R*)Val]$_5$–OMe (*n* = 5): Boc–[Aib–γ^4(*R*)Val]$_2$–OH (0.05 g, 0.15 mmol) was coupled to H–[Aib–γ^4(*R*)Val]$_3$–OMe, obtained by deprotecting Boc–[Aib–γ^4(*R*)Val]$_3$–OMe (0.116 g, 0.15 mmol) with 98% formic acid (2 mL) and then adding HATU (0.057 g, 0.15 mmol) and HOBt (0.023 g, 0.15 mmol). The reaction was worked up as described for Boc–Aib–γ^4(*R*)Val–OMe. Boc–[Aib–γ^4(*R*)Val]$_5$–OMe was obtained as a white solid (0.13 g, 73%), m.p. 251–252 °C. MS (ESI): 1193.0 $[M + H]^+$, 1215.0 $[M + Na]^+$, 1230.9 $[M + K]^+$.

Boc–[Aib–γ^4(*R*)Val]$_7$–OMe (*n* = 7): Boc–[Aib–γ^4(*R*)Val]$_4$–OMe (0.05 g, 0.051 mmol) was deprotected with 98% formic acid (0.5 mL) and was worked up as described for Boc–[Aib–γ^4(*R*)-Val]$_2$–OMe. The free base was added to a precooled solution of Boc–[Aib–γ^4(*R*)Val]$_3$–OH (0.03 g (0.051 mmol), obtained as described for Boc–[Aib–γ^4(*R*)Val]$_2$–OMe, in DCM (10 mL) and DMF (5 mL), and HATU (0.02 g, 0.051 mmol) and HOBt (0.008 g, 0.051 mmol) were added. The reaction mixture was allowed to attain room temperature and was stirred for 6–7 h. The reaction was worked up as described for Boc–Aib–γ^4(*R*)Val–OMe. Boc–[Aib–γ^4(*R*)Val]$_7$–OMe was obtained as a white solid (0.06 g, 73%), m.p. >300 °C (charred after 285 °C). MS (ESI): 1618.2 $[M + H]^+$, 1640.2 $[M + Na]^+$.

Boc-[Aib-γ^4(*R*)Val]$_8$-OMe (*n* = 8): Boc–[Aib–γ^4(*R*)Val]$_4$–OH (0.1 g, 0.1 mmol) was coupled with H–Aib–γ^4(*R*)Val–OH (0.088 g, 0.1 mmol) by using HATU (0.038 g, 0.1 mmol) and HOBt (0.015 g, 0.1 mmol). The reaction was worked up as described for Boc–Aib–γ^4(*R*)Val–OMe. Boc–[Aib–γ^4(*R*)Val]$_8$–OMe was obtained as a white solid (0.15 g, 82%), m.p. >300 °C. As the peptide was negligibly soluble in methanol, the solid was stirred in methanol for ca. 1 h and filtered through a sintered glass funnel to obtain pure peptide. MS (ESI): 1830 $[M + H]^+$, 1852 $[M + Na]^+$.

Supporting Information (see footnote on the first page of this article): CD and ESI-MS spectra; HPLC profiles; partial ROESY spectra for six- and 16-residue peptides.

Acknowledgments

This work was supported by a program grant from the Department of Biotechnology (DBT), India. B. D. was supported by the University grant numbers Commission (UGC), India (UGC-DSK Postdoctoral Fellowship).

[1] S. Hecht, I. Huc, *Foldamers: Structure, Properties, and Applications*, Wiley-VCH, Weinheim, Germany, **2007**.
[2] S. H. Gellman, *Acc. Chem. Res.* **1998**, *31*, 173–180.
[3] a) D. Seebach, A. K. Beck, D. J. Bierbaum, *Chem. Biodiversity* **2004**, *1*, 1111–1239; b) D. Seebach, J. Gardiner, *Acc. Chem. Res.* **2008**, *41*, 1366–1375; c) R. P. Cheng, S. H. Gellman, W. F. DeGrado, *Chem. Rev.* **2001**, *101*, 3219; d) P. G. Vasudev, S. Chatterjee, N. Shamala, P. Balaram, *Chem. Rev.* **2011**, *111*, 657–687; e) F. Bouillère, S. Thétiot-Laurent, C. Kouklovsky, V. Alezra, *Amino Acids* **2011**, *41*, 687–707; f) T. A. Martinek, F. Fülöp, *Chem. Soc. Rev.* **2012**, *41*, 687–702; g) C. M. Goodman, S. Choi, S. Shandler, W. F. DeGrado, *Nat. Chem. Biol.* **2007**, *3*, 252–262; h) G. Guichard, I. Huc, *Chem. Commun.* **2011**, *47*, 5933–5941.
[4] P. Balaram, *Biopolymers (Pept. Sci.)* **2010**, *94*, 733–741.
[5] a) E. A. Porter, X. Wang, M. A. Schmitt, S. H. Gellman, *Org. Lett.* **2002**, *4*, 3317–3319; b) T. J. Peelen, Y. Chi, E. P. English, S. H. Gellman, *Org. Lett.* **2004**, *6*, 4411–4414; c) M. Lee, T. L. Raguse, M. Schinnerl, W. C. Pomerantz, X. Wang, P. Wipf, S. H. Gellman, *Org. Lett.* **2007**, *9*, 1801–1804; d) W. S. Horne, L. M. Johnson, T. J. Ketas, P. J. Klasse, M. Lu, J. P. Moore, S. H. Gellman, *Proc. Natl. Acad. Sci. USA* **2009**, *106*, 14751–14756; e) S. H. Choi, I. A. Guzei, L. C. Spencer, S. H. Gellman, *J. Am. Chem. Soc.* **2009**, *131*, 2917–2924.
[6] a) L. Guo, Y. Chi, A. M. Almeida, I. A. Guzei, B. K. Parker, S. H. Gellman, *J. Am. Chem. Soc.* **2009**, *131*, 16018–16020; b) L. Guo, A. M. Almeida, W. Zhang, A. G. Reidenbach, S. H. Choi, I. A. Guzei, S. H. Gellman, *J. Am. Chem. Soc.* **2010**, *132*, 7868–7869; c) L. Guo, W. Zhang, A. G. Reidenbach, M. W. Giuliano, I. A. Guzei, L. C. Spenser, S. H. Gellman, *Angew. Chem.* **2011**, *123*, 5965; *Angew. Chem. Int. Ed.* **2011**, *50*, 5843–5846; d) L. Guo, W. Zhang, I. A. Guzei, L. C. Spencer, S. H. Gellman, *Org. Lett.* **2012**, *14*, 2582–2585.
[7] G. A. Lengyel, G. A. Eddinger, W. S. Horne, *Org. Lett.* DOI: 10.1021/ol4001125.
[8] a) K. Basuroy, A. Rajagopal, S. Ragothama, N. Shamala, P. Balaram, *Chem. Asian J.* **2012**, *7*, 1671–1678; b) K. Basuroy, V. Karuppiah, N. Shamala, P. Balaram, *Helv. Chim. Acta* **2012**, *95*, 2589–2603; c) P. G. Vasudev, R. Rai, N. Shamala, P. Balaram, *Biopolymers (Pept. Sci.)* **2008**, *90*, 138; d) P. G. Vasudev, S. Chatterjee, N. Shamala, P. Balaram, *Acc. Chem. Res.* **2009**, *42*, 1628–1639.
[9] T. Hintermann, K. Gademann, B. Jaun, D. Seebach, *Helv. Chim. Acta* **1998**, *81*, 983–1002.
[10] S. Hanessian, X. Luo, R. Schaum, S. Michnick, *J. Am. Chem. Soc.* **1998**, *120*, 8569–8570.
[11] a) G. V. M. Sharma, V. B. Jadhav, K. V. S. Ramakrishna, P. Jayaprakash, K. Narsimulu, V. Subash, A. C. Kunwar, *J. Am. Chem. Soc.* **2006**, *128*, 14657–14668; b) G. V. M. Sharma, N. Chandramouli, M. Choudhary, P. Nagendar, K. V. S. Ramakrishna, A. C. Kunwar, P. Schramm, H. J. Hofmann, *J. Am. Chem. Soc.* **2009**, *131*, 17335–17344.
[12] C. Baldauf, R. Günther, H. J. Hofmann, *J. Org. Chem.* **2006**, *71*, 1200–1208.
[13] a) K. Basuroy, B. Dinesh, N. Shamala, P. Balaram, *Angew. Chem.* **2012**, *124*, 8866; *Angew. Chem. Int. Ed.* **2012**, *51*, 8736–8739; b) K. Basuroy, B. Dinesh, N. Shamala, P. Balaram, *Angew. Chem. Int. Ed.* DOI: 10.1002/anie.201209324.
[14] S. Chatterjee, R. S. Roy, P. Balaram, *J. R. Soc. Interface* **2007**, *4*, 587–606.
[15] a) C. P. Rao, R. Nagaraj, C. N. R. Rao, P. Balaram, *FEBS Lett.* **1979**, *100*, 244–248; b) C. P. Rao, R. Nagaraj, C. N. R. Rao, P. Balaram, *Biochemistry* **1980**, *19*, 425–31.
[16] C. Toniolo, F. Formaggio, R. W. Woody, *Comprehensive Chiroptical Spectroscopy: Applications in Stereochemical Analysis of Synthetic Compounds, Natural Products, and Biomolecules*, John Wiley & Sons, Hoboken, **2012**, vol. 2, p. 499–544.
[17] C. Toniolo, F. Formaggio, *Comprehensive Chiroptical Spectroscopy: Applications in Stereochemical Analysis of Synthetic Compounds, Natural Products, and Biomolecules*, John Wiley & Sons, Hoboken, **2012**, vol. 2, p. 545–574.
[18] A. Bandyopadhyay, H. N. Gopi, *Org. Lett.* **2012**, *14*, 2770–2773.

Received: February 20, 2013
Published Online: May 14, 2013

